

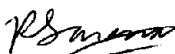
Spectral Analysis of the Black Hole Candidate 4U 1630-47

Rishik Saxena  
ERULF Program  
University of California at Berkeley  
Stanford Linear Accelerator Center  
Menlo Park, California

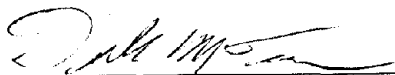
08/14/02

This paper was prepared in partial fulfillment of the requirements of the DOE Energy Research Undergraduate Laboratory Fellowship under the direction of Derek Tournear in Group K at Stanford Linear Accelerator Center.

Participant:

  
\_\_\_\_\_  
Signature

Research Advisor:

  
\_\_\_\_\_  
Signature

## Table of Contents

Abstract	1
Introduction	2
Theory	3
Data Analysis	5
Results	7
Conclusion	8
Acknowledgements	11
References	12
Figures	14

## Abstract

We performed spectral analysis on the 1999 X-ray outburst of the soft X-ray transient black hole candidate (BHC) 4U 1630-47, in order to learn about physical processes (such as changes in inner disk radius of the accretion disk) that manifest themselves as changes of state. This source goes through an outburst every 600 – 690 days, which is a very short time period compared with other transient X-ray sources. The overall shape of the outburst's light curve was very similar to that of the 1996 outburst, but noticeably different from that of the 1998 outburst. We fitted 47 observations of the outburst to a model consisting of a disk blackbody, inverse Comptonization power law, and Gaussian component, multiplied by an absorption constant and an overall normalization constant. We found that the BHC progressed from a low state to high, and then back to low during its outburst. This pattern is common to persistent sources, not transient sources. We also found that when the source is in the low state, the flux and hardness are anticorrelated, as is predicted by theory. However, when 4U 1630-47 is in the high state, it is unclear whether or not the flux and hardness are correlated as theory says they should be.

## 1. Introduction

4U 1630-47 is a soft X-ray transient in a low-mass binary system (Kuulkers et al. 1997). Previous spectral and timing analyses performed on the source show that it is most likely a black hole (White et al. 1984; Parmar et al. 1986; Kuulkers et al. 1997), and thus 4U 1630-47 is known as a black hole candidate (BHC). Normally, such sources experience recurrent X-ray outbursts every 10 – 50 years (Parmar et al. 1995), but 4U 1630-47 is unusual in that it goes through an outburst every 600 – 690 days. This feature allows us to collect data from 4U 1630-47 frequently, which makes it a valuable source of information on black hole candidates.

Based on the characteristics of X-ray emission during an outburst, a BHC can be classified as being in a low, intermediate, or high state (in order of decreasing hardness and increasing flux, where hardness is defined as the ratio of high-energy X-rays to low-energy X-rays [Dieters et al. 2000]). These states reflect the rate of accretion of matter into the black hole; according to current theoretical models, if the rate of accretion is increasing, then the black hole will progress through the states in the order given above, but if the rate is decreasing, the order will be reversed (Dieters et al. 2000). Thus, changes in the energy spectra of a BHC (representing changes in hardness) can give us information about the physical properties of an accreting black hole.

To perform spectral analysis on 4U 1630-47, we used data from the RXTE satellite in the energy range of 3 – 264 keV (Bradt 1993). Using XSPEC, we analyzed energy spectra of the source. These spectra were fit to a model; in the case of 4U 1630-47, the best-fitting model is a combination of an inverse Comptonization power law component developed by L. Titarchuk (Titarchuk 1994), a Gaussian component, and a disk blackbody component. The best-fit parameters to these spectra correspond to physical properties of the source, such as its inner disk

temperature and plasma temperature. Observing how these properties change with time during the outburst as well as how the overall spectrum evolves gives us clues about the physical processes the source is undergoing.

The two most recent outbursts of 4U 1630-47 for which we have data occurred in 1998 and 1999. The former outburst has been studied in detail, but the 1999 outburst has not, and this was the goal of our project. Our results will be helpful in determining why 4U 1630-47 has such frequent outbursts, as well as determining what accounts for changes in its state. This information should facilitate the formulation of better theoretical models of the source and the processes that it is undergoing (such as methods of energy transfer) which are responsible for the transitions in state.

## **2. Theory**

A black hole in a binary system pulls matter away from its companion and the surrounding plasma (see Figure 1). This matter accumulates around the black hole in a disk (known as an accretion disk) which spirals inward toward the black hole. As the accreting matter spirals inward, it heats up due to compression (Carrol & Ostlie 1996) and friction, causing it to emit a blackbody spectrum. Some of these blackbody photons, called seed photons, are Compton upscattered by relativistic electrons in the surrounding plasma, and this results in the energy spectrum consisting not only of a blackbody spectrum but also a high-energy tail modeled by a power law. The ratio of high-energy X-rays to low-energy X-rays (hardness) changes during an outburst and defines the state of the black hole. Furthermore, within each state, the correlation (or anticorrelation) between the hardness and the flux is a direct consequence of the physics of the accretion disk and surrounding plasma, as will be discussed later.

At the beginning of an outburst, a black hole is in a low state, defined by a hard energy spectrum and low flux. It then progresses through an intermediate and high state, each state being characterized by a softer spectrum and higher flux. The high state thus corresponds to the peak of the outburst. This progression from low to high state also corresponds to an increasing accretion rate and a decreasing inner disk radius. Following the peak of the outburst, the spectrum becomes harder again, and the flux decreases as the outburst fades from the high state down to intermediate, and finally to the low state.

It has been found in the past that when a black hole is in a soft (high) state, the hardness and flux are correlated (Zdziarski et al. 2002). This can be explained by noting the following. When a black hole is in a soft state, it is believed that the inner radius of the accretion disk extends down to the last stable orbit (Meyer et al. 2001). Thus, the temperature of the inner radius is very hot and the contribution of its blackbody emission to total energy dominates over the contribution from the plasma. Consequently, changes in the energy of the accretion disk (rather than the energy of the plasma) dictate the behavior of the spectrum. As a result, as the blackbody flux increases, the blackbody spectrum shifts toward higher energies, creating a harder spectrum.

On the other hand, in a hard (low) state, the hardness and flux are found to be anticorrelated. When a black hole is in this state, the inner radius of the accretion disk is far away from the last stable orbit (Meyer et al. 2001), so the temperature of the inner disk radius is not as hot. Thus, the relative contribution of the blackbody emission to total energy is low, and consequently, changes in plasma energy dictate the behavior of the spectrum. As blackbody flux increases, more electrons in the plasma are involved in Compton upscattering, thereby causing

an overall reduction in the thermal energy of the electrons; this causes the high-energy flux to reduce, resulting in a decrease in the hardness of the spectrum.

### **3. Data Analysis**

#### **3.1 Data**

We looked at a total of 47 RXTE observations of 4U 1630-47. The observations were, on average, 2.8 days apart, spanning from May 8, 1999 to Sept. 15, 1999, and each observation was, on average, 13.9 minutes long. During these observations, three instruments on the RXTE satellite (PCA, HEXTE A, and HEXTE B) recorded the time and energy information of incident photons. The energy ranges of the PCA, HEXTE A, and HEXTE B instruments are 0.04 – 119.4 keV, 0.1 – 273.6 keV, and 0.1 – 272.5 keV, respectively (Bradt et al. 1993); however, we only looked at the ranges 3 – 28 keV for PCA and 28 – 264 keV for HEXTE. Using the standard FTOOLS package (version 5.2), we processed the raw data and prepared it for use with the spectrum-analyzing program XSPEC (Arnaud 1996).

#### **3.2 Analysis**

We used XSPEC on each observation to load the PCA and HEXTE data and to load relevant background and correction information. The model we used for fitting was a sum of a disk blackbody component, an inverse Comptonization power law component (comptt), and a Gaussian component, multiplied by an overall constant and an absorption constant (see Figure 2). The disk blackbody component represents blackbody emission from the accretion disk, the comptt component represents Compton-upscattered blackbody photons in the hot surrounding plasma (Titarchuk 1994), and the Gaussian component represents iron emission around 6 keV. For each of the three data sets (one for each instrument), there were a total of 13 parameters: the

constant factor, the hydrogen column density ( $nH$ ), the temperature at the inner disk radius ( $T_{in}$ ), the disk blackbody component normalization, the redshift, the soft photon temperature ( $t_0$ ), the plasma temperature ( $kT$ ), the plasma optical depth ( $\tau_{up}$ ), the geometry switch (which sets either spherical or disk geometry), the comptt normalization, the Gaussian line energy, the Gaussian line width, and the Gaussian normalization. We fixed the hydrogen column density at  $6.55 \times 10^{22}$  atoms/cm<sup>2</sup> (Parmar et al. 1986), the redshift at 0, and the PCA constant factor at 1.0. The geometry switch was already automatically frozen at 1.0, representing disk geometry. All other parameters were allowed to float. The anneal method was used in performing all the fits except the last, which was performed using the Levenberg-Marquardt method (this was necessary in order to calculate errors in the parameters).

As previously mentioned, we restricted the energy ranges of the PCA and HEXTE data for our use. We also ignored channels which had previously been labeled as “bad,” meaning that the instrument response in those channels cannot be calculated accurately. A systematic error of 2% was used. Initially, we had used the PCA and HEXTE background files only for background correction, but we noticed prominent bumps in the HEXTE data from 50 to 100 keV on some of the plots, indicating that the HEXTE background was under-subtracted. So, we used the background files also as correction files for the HEXTE data.

Using XSPEC, we found the fluxes for each instrument as well as those for each individual additive model component (the latter was done by setting the normalizations of two of the additive components to zero and having XSPEC find the remnant flux of the third component). All of these fluxes were calculated after setting the hydrogen column density to zero to eliminate effects of absorption. We outputted all of this information, along with the best-fit parameters and plots, to files which we subsequently analyzed using Microsoft Excel<sup>®</sup>.

#### 4. Results

Out of a total of 47 observations, 9 had reduced chi-squares above 2.0. These were ignored in our following analysis. Additionally, the very last observation was ignored due to an unusually high hardness. The rest of the reduced chi-squares ranged from 0.8 to 1.9.

Our best-fit parameters for the fits with acceptable reduced chi-squares are shown in Table 1. The All Sky Monitor (ASM) light curve of 4U 1630-47 from 1996 up to the present is shown in Figure 3. A PCA light curve of the entire 1999 outburst is shown in Figure 4. An example of a fitted energy spectrum is shown in Figure 5.

We defined a hardness ratio by [average HEXTE comptt flux / PCA disk blackbody flux]. When this hardness ratio is plotted against the PCA count rate, it appears that the harder emission occurs only at lower PCA count rates (see Figure 6).

Figure 7 (top) shows the temperature at the inner disk radius versus time. The very first observation shows a temperature of  $8 \times 10^{-3}$  keV (error unknown), which then jumps up to  $1.23 \pm 0.0156$  keV in the next observation, which is 4.7 days later. It then decreases to a local minimum of  $1.16 \pm 0.0053$  keV, after which it rises to a maximum of  $1.40 \pm 0.0029$  keV at the peak of the outburst, following which it decreases steadily until leveling out around an average temperature of  $0.05 \pm 0.002$  keV. The lowest temperature we see, then, is that of the very first observation,  $8 \times 10^{-3}$  keV. However, XSPEC was unable to calculate the error on this temperature, and so this number may be unreliable.

In Figure 7 (middle) we have shown the hardness ratio plotted versus time, and below that we show again the PCA light curve for comparison purposes. It is evident here that the spectrum goes from hard at the beginning of the outburst to soft at the peak, and then increases in

hardness towards the very end of the outburst. The softest spectrum coincides with the peak of the outburst.

In Figures 8 and 9 we have compared the 1999 outburst to the one in 1998. We show some fitted spectra from the initial rise of both outbursts in Figure 8, and some from the peak of both outbursts in Figure 9. (The 1998 spectra are from Trudolyubov et al. 1999.) We have also shown the fitted spectrum from the very last 1999 observation in Figure 10 for comparison with the other 1999 spectra (unfortunately, Trudolyubov et al. did not provide spectra for the end of the 1998 outburst). From Figure 11 it is evident that during the 1998 outburst, the emission became softer throughout the outburst. This is very different from the 1999 outburst, during which the emission changed from hard to soft and then back to hard.

## **5. Conclusion**

### **5.1 Discussion**

The 1999 outburst occurred much earlier than was predicted (Trudolyubov et al. 1999). It has been suggested that since the period of recurrence of outbursts from 4U 1630-47 is not well-defined, the outbursts may not be related to the binary orbit (Trudolyubov et al. 1999). The 1999 outburst also had a considerably lower peak flux than did both the 1996 and 1998 outbursts, as can be seen in Fig. 3. In terms of shapes of the light curves, the 1999 outburst looks very similar to the 1996 outburst, but very different from the 1998 outburst. The 1998 outburst is of the fast-rise-exponential-decay (FRED) type, whereas the 1999 outburst is not.

The transformation from a hard spectrum at the beginning of the outburst to soft and then back to hard at the end of the outburst indicates transitions from a low state to the high state and then back to the low state, using the general rule that transitions from lower states to higher states

manifest themselves as increasingly soft spectra, and transitions from higher states to lower states manifest themselves as increasingly hard spectra. As mentioned earlier, the accretion rate of matter around the BHC is also related to changes in state; a progression from a low state to high state indicates an increasing accretion rate. Thus, during the 1999 outburst, the accretion rate increases as 4U 1630-47 progresses through its outburst to the high state, and thereafter decreases as the outburst dies down.

At the beginning of the outburst, the count rate is 1300 counts/sec. This subsequently increases towards a peak of 2700 counts/sec as 4U 1630-47 goes from the low (hard) to high (soft) state. The spectrum is softest right around the peak intensity (see Figure 7), as is expected. Following the peak, the count rate decreases as the outburst fades out and the spectrum becomes harder again.

During the rise and fall of the outburst, when 4U 1630-47 is in the low state, the intensity and hardness are seen to be anticorrelated (see Figure 7), as is predicted by theory. However, during the peak of the outburst, when 4U 1630-47 is in the high state, it is unclear whether or not the intensity and hardness are correlated as theory predicts.

The very high blackbody normalizations and low inner disk radius temperatures seen towards the end of the outburst and for the very first observation (see Table 1) are consistent with theory. Recall that the black hole is in the low state at the beginning and end of the outburst. According to the theoretical model described in the theory section, the inner disk radius of the accretion disk is far away from the last stable orbit during the low state. This is consistent with the blackbody normalizations being high since these normalizations are in fact proportional to the square of the inner disk radius (Oosterbroek et al. 1998). And, since the inner radius is far from the last stable orbit, its temperature is low. The low temperatures during the

low states can be seen clearly in Figure 7 (top). Accordingly, a glance at this same figure shows clearly that at the peak of the outburst, the temperature of the inner disk radius is at its maximum. This fits the theory that in the high state, the inner radius extends down to the last stable orbit, causing the temperature there to be very high.

Our definition of hardness explains why we obtained an unusually high hardness for the last observation. At the end of the outburst, when the black hole is in the low state, the inner disk radius is far away from the last stable orbit and its temperature is low. The resultant blackbody flux is barely detectable, giving us a very high hardness ratio.

Trudolyubov et al. found that there was a “very hard state dominated by a hard power law” near the peak of the 1998 outburst, an occurrence that is common for X-ray transients. We, however, did not notice such an occurrence in the 1999 outburst. The 1999 outburst follows a well-defined hard-soft-hard transition, as was seen in the 1996 outburst and is also seen in persistent sources such as Cyg X-1 (Trudolyubov et al. 1999). Thus, our work supports Trudolyubov’s conclusion that the behavior of 4U 1630-47 is similar to both that of transient sources and persistent sources.

## **5.2 Proposals for Future Analysis**

In the future, timing analysis must be done on 4U 1630-47 to search for timing irregularities such as quasi-periodic oscillations (QPO’s). These were present in the 1998 outburst (Trudolyubov et al. 1999) and are interesting because they usually reflect instabilities in the accretion disk.

It would also be interesting to perform the same kind of spectral analysis that we performed using data from the USA satellite. This satellite has an energy range of 1 – 15 keV.

Additionally, it might be useful to consider smaller energy ranges when defining a hardness ratio. This would also make our analysis more consistent with that of the 1998 outburst.

Finally, spectral and timing analyses should be performed on the latest outburst of 4U 1630-47, which occurred in 2001. It will be interesting to compare the results with those of previous outbursts.

### **Acknowledgements**

I thank the U. S. Department of Energy for giving me the opportunity to participate in the summer 2002 ERULF program at Stanford Linear Accelerator Center (SLAC). I would like to thank my mentor Derek Tournear for all his help and advice. I am also thankful to Warren Focke and Kaice Reilly for their help, and to Elliot Bloom for allowing me to work in his group here at SLAC.

I thank the Department of Energy and SLAC for creating, organizing, and funding this program, and the National Science Foundation for its help in funding the program as well.

## References

- Arnaud, K.A. (1996). XSPEC: The first ten years. ASP Conf. Ser. 101: Astronomical Data Analysis Software and Systems, 5, 17.
- Bradt, H.V., Rothschild, R.E., & Swank, J.H. (1993). X-ray timing explorer mission. Astronomy and Astrophysics Supplement Series, 97, 355-360.
- Carroll, B.W., Ostlie, D.A. (1996). An Introduction to Modern Astrophysics. Reading: Addison-Wesley.
- Dieters, S.W., Belloni, T., Kuulkers, E., Woods, P., Cui, W., Zhang, S.N., Chen, W., van der Klis, M., van Paradijs, J., Swank, J., Lewin, W.H.G., & Kouveliotou, C. (2000). The timing evolution of 4U 1630-47 during its 1998 outburst. The Astrophysical Journal, 538 (1), 307-314.
- Kuulkers, E., Parmar, A.N., Kitamoto, S., Cominsky, L.R., & Sood, R.K. (1997). Complex outburst behavior from the black-hole candidate 4U 1630-47. Monthly Notices of the Royal Astronomical Society, 291 (1), 81-90.
- Kuulkers, E., van der Klis, M., Parmar, A.N. (1997). Evidence for an anomalous state in the black hole candidate 4U 1630-47. The Astrophysical Journal, 474, L47.
- Meyer, F., Liu, B.F., & Meyer-Hofmeister, E. (2001). Black hole X-ray binaries: a new view on soft-hard spectral transitions. Astronomy and Astrophysics, 354, L67-L70.
- Oosterbroek, T., Parmar, A.N., Kuulkers, E., Belloni, T., van der Klis, M., Frontera, F., & Santangelo, A. (1998). The 1998 outburst of the X-ray transient 4U 1630-47 observed with BeppoSAX. Astronomy and Astrophysics, 340, 431-436.
- Parmar, A.N., Angelini, L., & White, N.E. (1995). Periodic outbursts from the ultrasoft X-ray transient 4U 1630-47. The Astrophysical Journal, 452, L129.

- Parmar, A.N., Stella, L., & White, N.E. (1986). The evolution of the 1984 outburst of the transient X-ray source 4U 1630-47. The Astrophysical Journal, 304, 664.
- Titarchuk, L. (1994). Generalized Comptonization models and application to the recent high-energy observations. The Astrophysical Journal, 434, 570-586.
- Trudolyubov, S.P., Borozdin, K.N., & Priedhorsky, W.C. (1999). RXTE observations of 4U 1630-47 during the peak of its 1998 outburst. Monthly Notices of the Royal Astronomical Society, 322 (2), 309.
- White, N.E., Kaluzienski, J.L., & Swank, J.H. (1984). Woosley, S.E., ed., Proc AIP Conf. 115, High Energy Transients in Astrophysics. AIP, New York, 31.
- Zdziarski, A.A., Poutanen, J., Paciesas, W.S., & Wen, L. (2002). Understanding the long-term spectral variability of Cygnus X-1 with BATSE and ASM observations. *Apj*, in press.



**Figure 1.** An accreting black hole pulling matter away from its companion star.

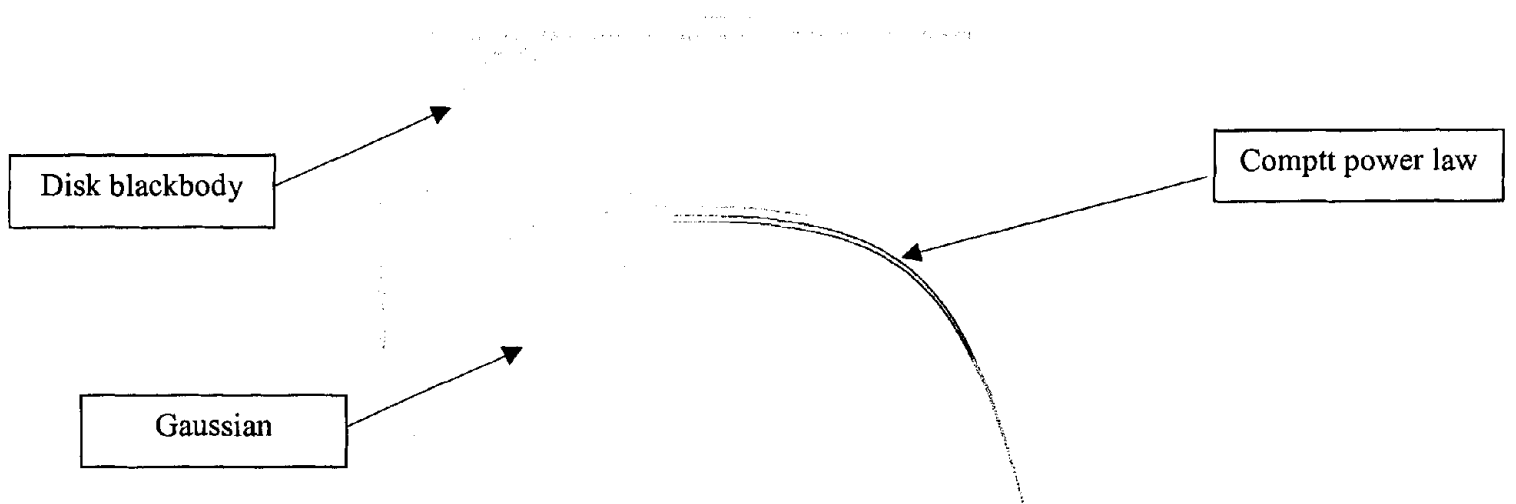


**Figure 2.** Components of the model we used to fit the data.

Time (MJD)	Diskbb $T_{in}$ (keV)	Diskbb Norm	Comptt $t_0$ (keV)	Comptt $kT$ (keV)	Comptt $\tau_{aup}$	Comptt Norm	Gaussian Line E (keV)	Gaussian Sigma	Gaussian Norm	HEXTE A Constant Factor	HEXTE B Constant Factor
51306.1	0.008	7.8E+23	5.3E-02	22.2	2.14	7.2E-02	6.2648	0.499	3.1E-03	0.801	0.800
51310.8	1.234	1.2E+02	9.2E-03	36.5	0.87	4.3E-01	6.4	0.012	1.6E-04	0.800	0.800
51311.6	1.266	1.3E+02	4.7E-03	110.4	0.32	1.1E-01	5.8	0.648	1.4E-03	0.800	0.863
51316.9	1.205	2.1E+02	4.6E-03	41.8	1.03	1.8E-01	6.0426	0.648	4.1E-03	-0.940	0.800
51318.9	1.171	2.1E+02	1.5E-02	40.1	0.91	1.5E-01	6.0036	0.582	5.3E-03	0.800	0.800
51320.3	1.216	2.0E+02	1.3E-02	41.1	1.03	1.0E-01	5.9542	0.585	7.3E-03	0.800	0.801
51322.0	1.224	2.0E+02	2.7E+00	5.6	5.87	9.7E-03	5.8	0.648	5.0E-03	0.950	0.950
51324.3	1.160	2.4E+02	2.9E-03	43.0	1.06	1.7E-01	5.8001	0.647	8.1E-03	0.800	0.800
51328.5	1.166	2.6E+02	1.1E-02	43.7	1.01	5.5E-02	6.048	0.495	6.4E-03	0.801	0.811
51330.0	1.197	2.5E+02	8.1E-03	38.7	1.06	1.5E-01	5.9891	0.647	9.0E-03	0.800	0.800
51332.6	1.198	2.6E+02	5.7E-03	46.1	0.95	1.0E-01	5.9897	0.647	8.5E-03	0.800	0.800
51337.2	1.238	2.6E+02	8.5E-03	39.8	0.89	1.9E-01	5.8228	0.648	1.3E-02	0.800	0.800
51344.0	1.257	2.9E+02	5.1E-02	45.6	0.78	3.0E-02	6.0276	0.598	1.3E-02	0.800	0.874
51346.7	1.403	1.9E+02	3.9E+00	123.4	0.03	5.1E-04	5.8	0.648	2.1E-02	0.949	0.800
51347.7	1.281	2.7E+02	3.2E-02	61.8	0.49	1.0E-01	6.0184	0.646	2.5E-02	0.800	0.800
51348.2	1.286	2.7E+02	7.3E-03	56.5	0.79	9.3E-02	5.9862	0.648	1.7E-02	0.800	0.800
51351.2	1.281	2.8E+02	4.8E-03	45.5	0.81	2.5E-01	6.1183	0.648	1.5E-02	0.800	0.800
51365.4	1.269	2.4E+02	4.0E-03	50.4	0.75	3.7E-01	6.1922	0.440	7.4E-03	0.801	0.800
51377.3	1.085	1.7E+02	8.1E-03	41.9	0.86	2.0E-01	6.4	0.000	2.4E-04	0.800	0.800
51380.8	1.055	1.5E+02	7.0E-03	43.5	0.89	1.2E-01	6.3999	0.645	7.9E-07	0.800	0.800
51391.6	0.988	1.6E+02	5.3E-03	35.7	0.95	3.8E-01	6.3998	0.397	3.9E-04	0.801	0.800
51382.7	1.053	1.0E+02	5.8E-03	46.3	0.83	1.4E-01	6.3999	0.582	1.1E-07	0.800	0.800
51383.7	1.013	1.0E+02	7.3E-03	40.4	0.78	2.8E-01	6.3989	0.645	6.9E-07	0.802	0.800
51384.7	0.825	2.8E+02	1.8E-02	26.5	1.69	9.7E-02	6.3999	0.646	2.2E-03	0.800	0.800
51386.6	0.736	4.1E+02	1.1E+00	26.9	1.38	4.7E-03	6.4	0.648	1.8E-03	0.800	0.800
51387.6	0.723	3.5E+02	2.0E-02	25.6	1.42	1.2E-01	6.3995	0.517	1.7E-03	0.832	0.949
51390.1	0.654	4.3E+02	1.7E-02	27.2	1.28	1.2E-01	6.3993	0.580	1.5E-03	0.800	0.801
51394.8	0.054	2.8E+23	1.3E-02	30.2	1.38	7.6E-02	6.4	0.006	5.0E-04	0.950	0.801
51395.5	0.052	6.5E+23	1.6E-02	31.1	1.31	5.5E-02	6.4	0.061	4.1E-04	0.801	0.949
51397.2	0.054	1.3E+23	4.2E-01	49.7	0.55	2.1E-03	6.3999	0.000	2.2E-04	0.950	0.800
51398.2	0.054	8.2E+23	4.2E-03	32.8	1.24	9.5E-02	6.4	0.092	2.1E-04	0.950	0.800
51400.1	0.055	2.2E+23	2.7E-02	12.4	2.29	8.4E-02	6.4	0.001	3.3E-04	0.944	0.800
51400.7	0.054	1.7E+23	1.2E-02	26.8	1.46	4.8E-02	6.3999	0.041	3.9E-04	0.805	0.800
51402.0	0.051	9.7E+23	2.0E-02	26.1	0.99	8.0E-02	6.3996	0.026	2.1E-04	0.950	0.801
51404.0	0.056	1.2E+23	2.0E-02	24.9	1.24	5.3E-02	6.3995	0.004	2.9E-04	0.937	0.801
51406.3	0.059	1.2E+22	2.8E-02	25.0	1.21	4.1E-02	6.4	0.245	4.5E-04	0.801	0.800
51408.0	0.050	9.8E+23	2.4E-02	28.9	0.65	1.1E-01	6.4	0.328	3.3E-04	0.946	0.802
51436.1	0.042	6.8E+23	1.9E-02	30.8	1.68	2.2E-02	6.3948	0.498	1.1E-03	0.803	0.801

**Table 1.** Best-fit parameters for fits with acceptable ( $< 2.0$ ) reduced chi-squares.  $T_{in}$  is the temperature of the inner disk radius,  $t_0$  is the soft photon temperature,  $kT$  is the plasma temperature, and  $\tau_{aup}$  is the plasma optical depth.

# X1630-472 ASM Lightcurve

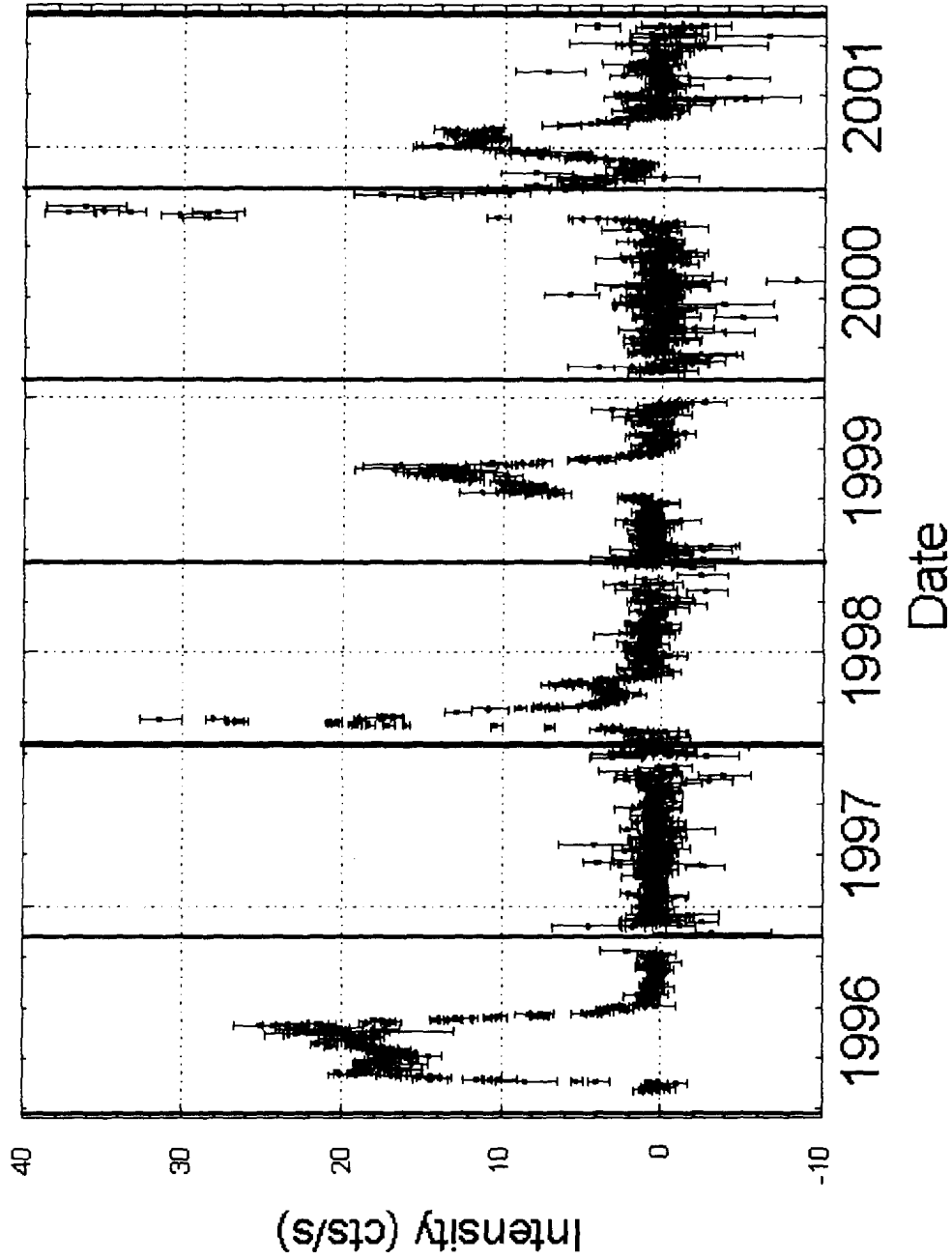


Figure 3. ASM light curve showing 1996, 1998, 1999, and 2001 outbursts of 4U 1630-47.

# X1630-472 ASM Lightcurve

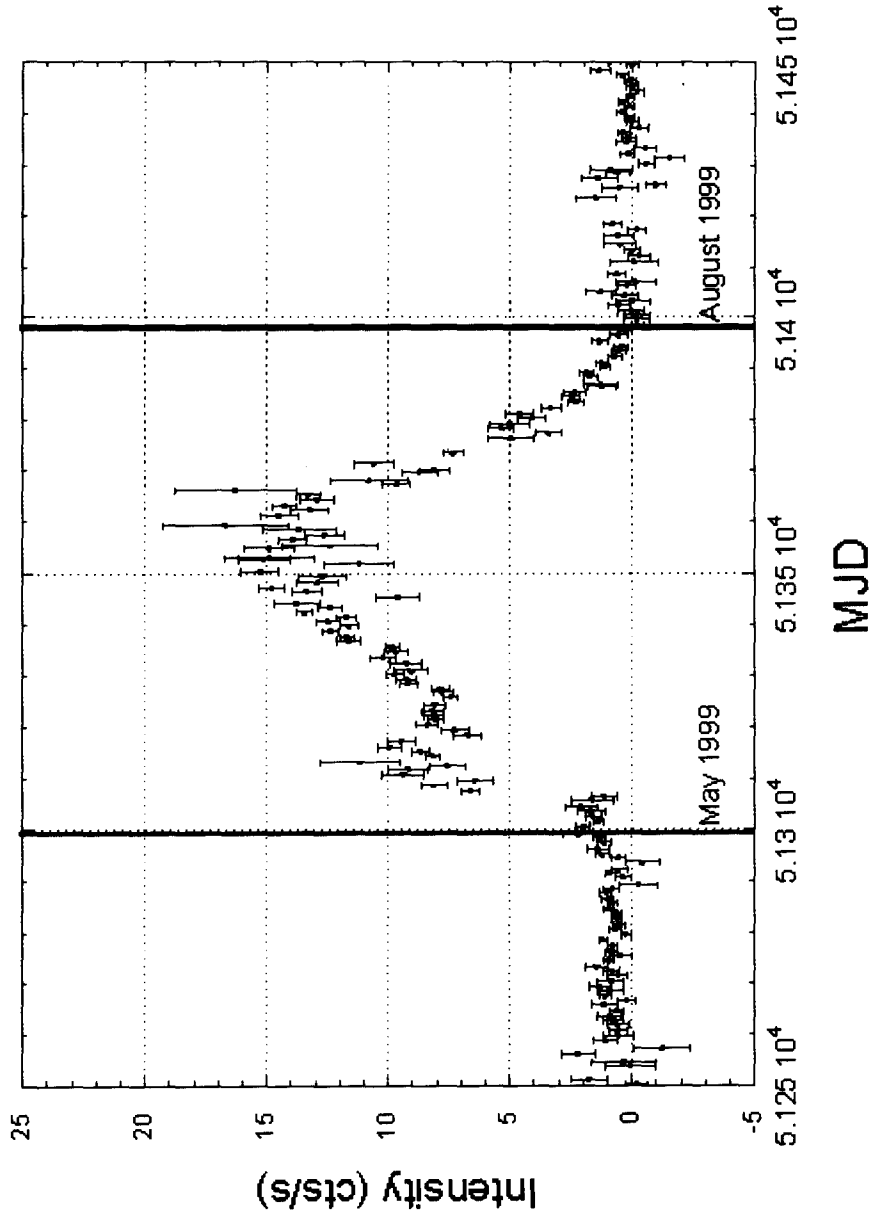
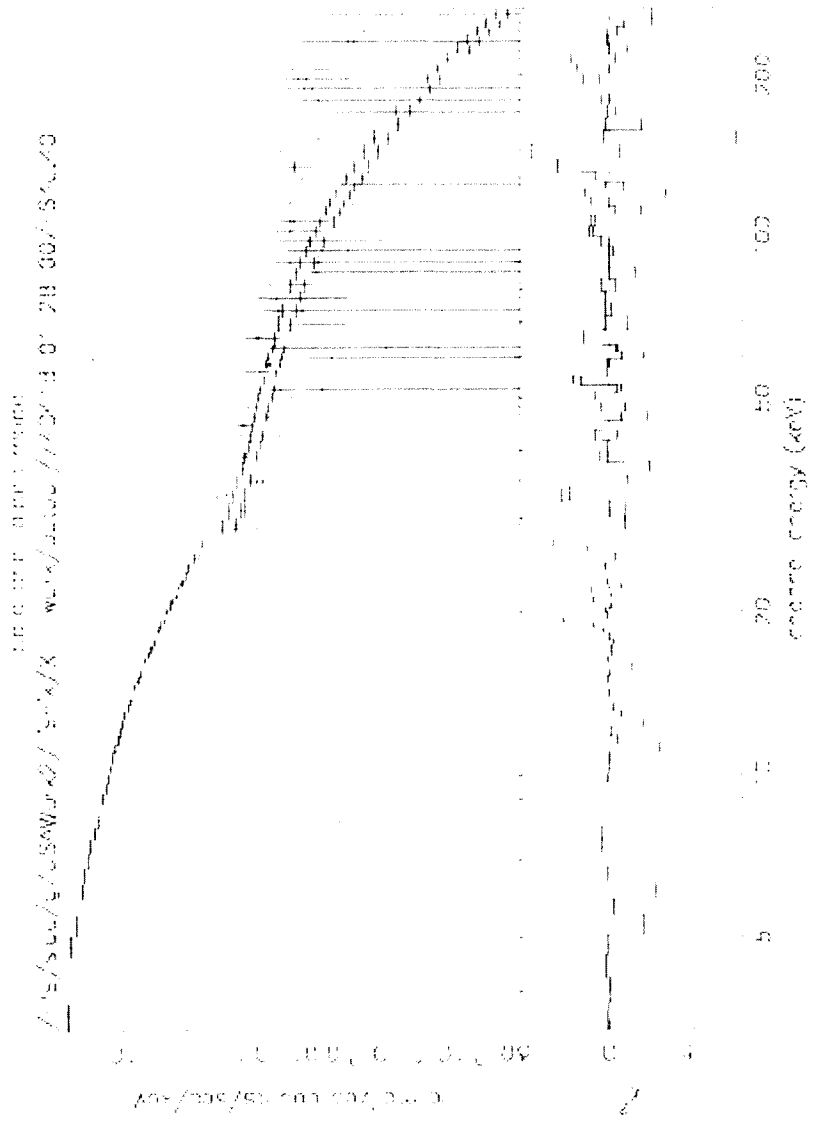


Figure 4. PCA light curve of 1999 outburst of 4U 1630-47.



9 Aug 2000 11:15

**Figure 5. Good fit to energy spectrum (reduced chi-squared = 1.01).**



### 4U 1630-472 1999 Outburst

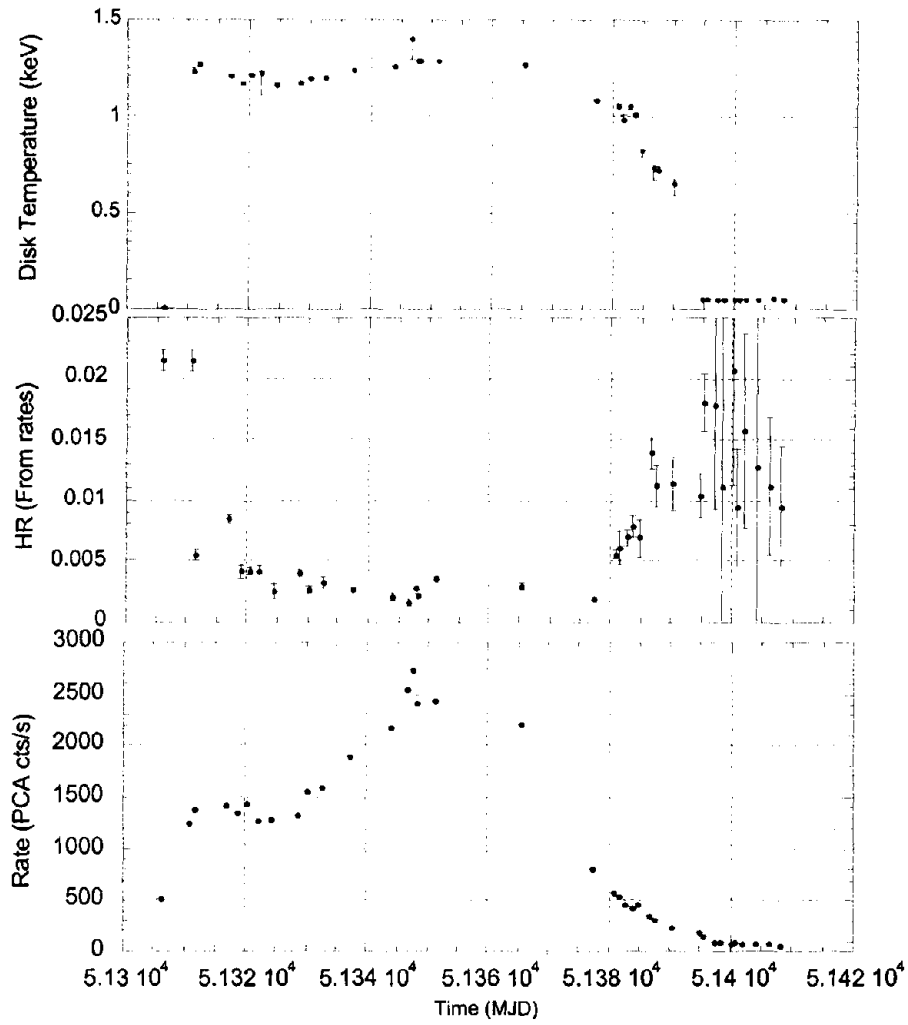
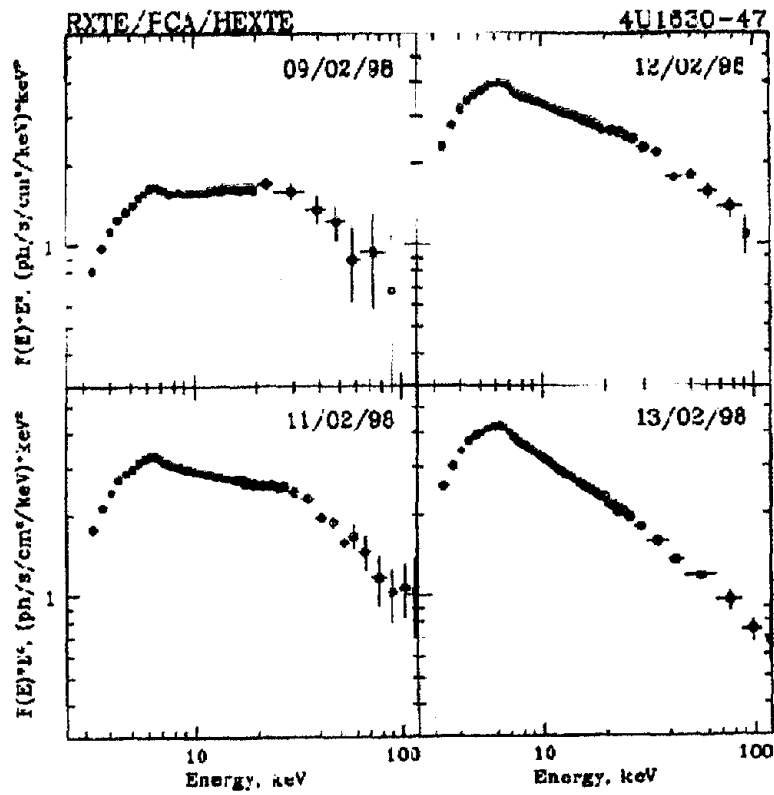


**Figure 7.** Inner disk radius temperature, hardness ratio, and PCA count rate as functions of time.

### INITIAL RISE OF 1998 OUTBURST



### INITIAL RISE OF 1999 OUTBURST

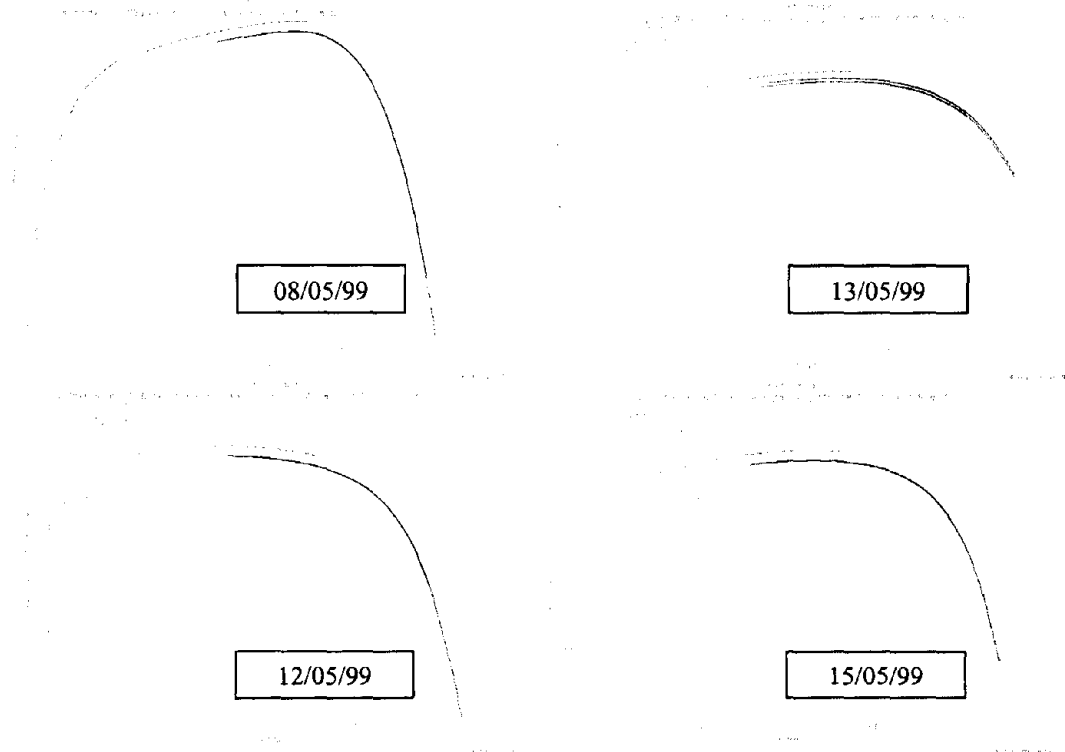
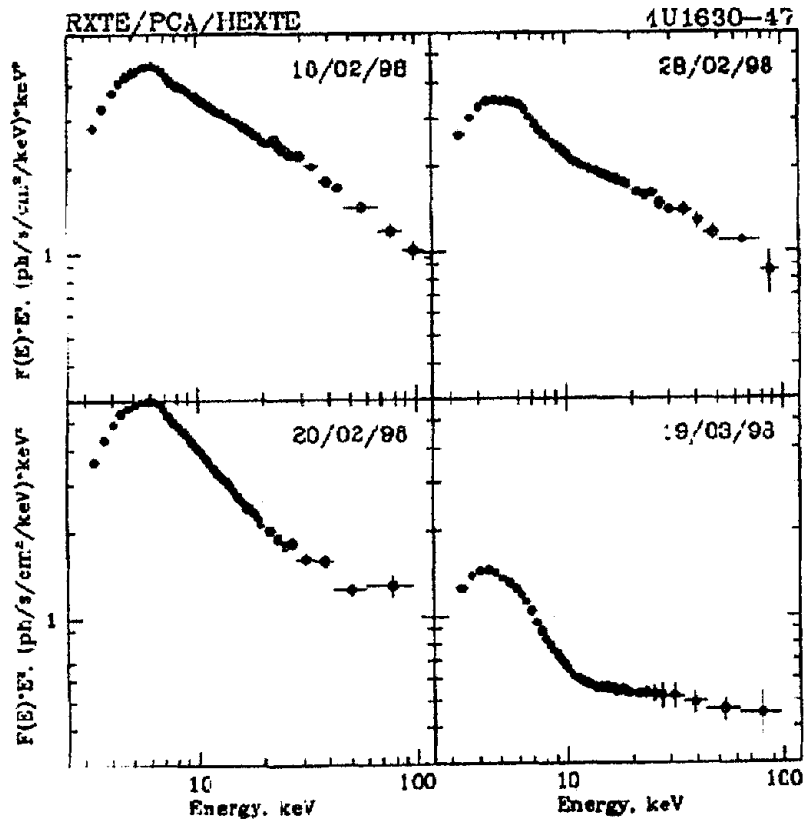


**Figure 8.** Comparison of rise of 1998 outburst to rise of 1999 outburst. (The 1998 spectra are from Trudolyubov et al. 1999).

### PEAK OF 1998 OUTBURST



### PEAK OF 1999 OUTBURST

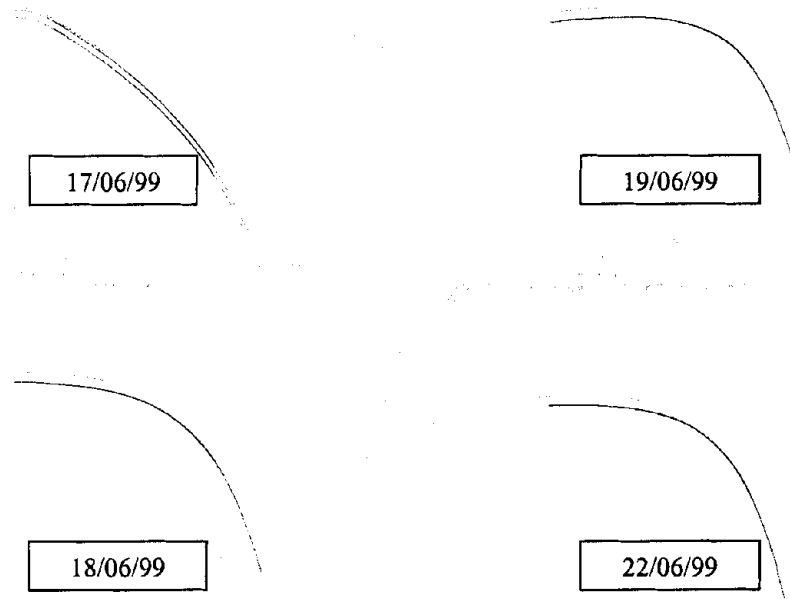


**Figure 9.** Comparison of peak of 1998 outburst to peak of 1999 outburst. (The 1998 spectra are from Trudolyubov et al. 1999).

# END OF 1999 OUTBURST

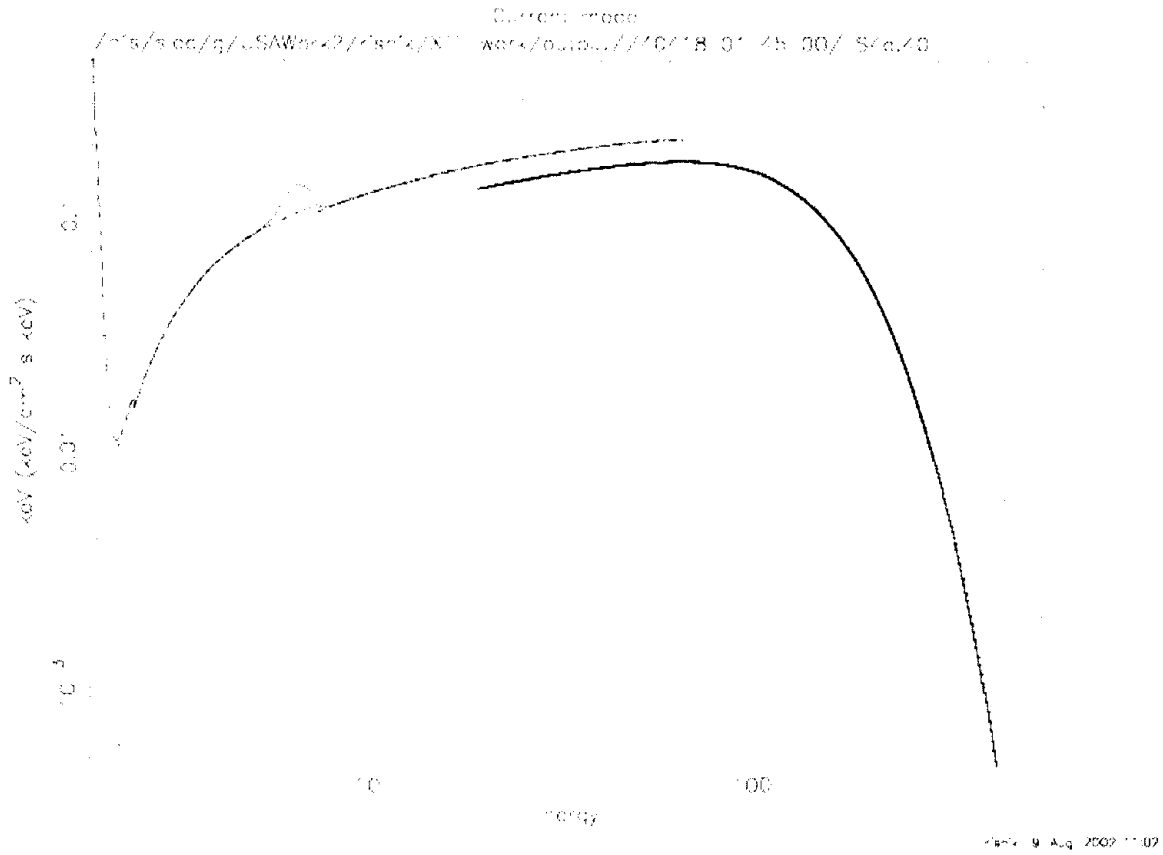


**Figure 10. End of 1999 outburst.**

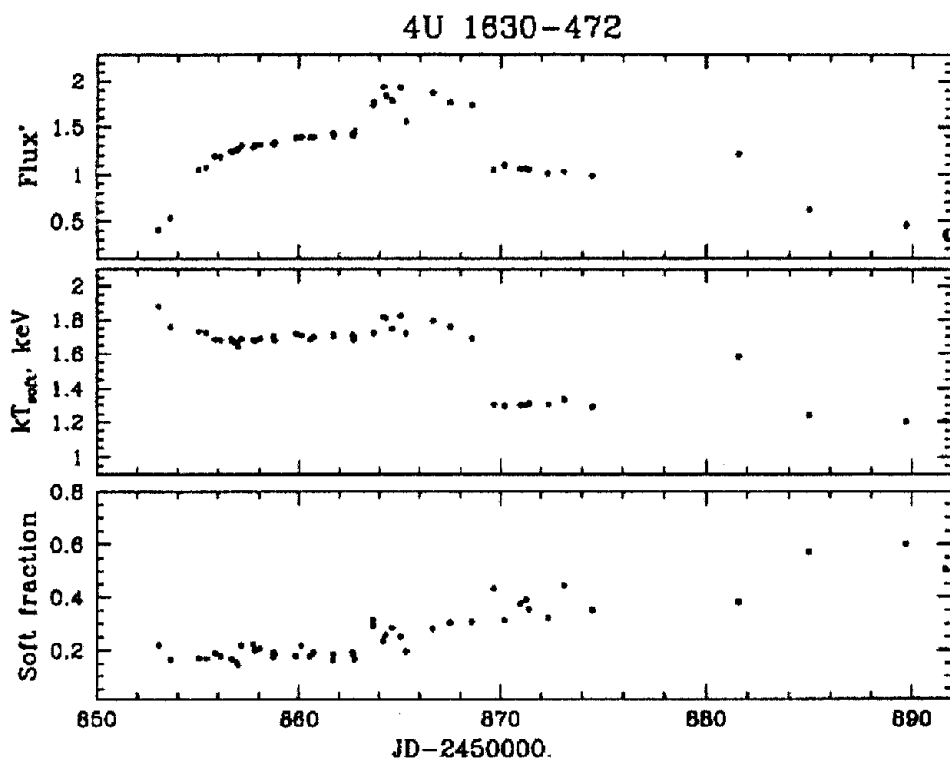


Figure 11. Flux, kT, and soft fraction of 1998 burst, taken from Trudolyubov et al. 1999.